ARMY RESEARCH LABORATORY

Model-Based Radar Power Calculations for Ultra-Wideband (UWB) Synthetic Aperture Radar (SAR)

by Traian Dogaru

ARL-TN-0548 **June 2013**

NOTICES

Disclaimers

The findings in this report are not to be construed as an official Department of the Army position unless so designated by other authorized documents.

Citation of manufacturer's or trade names does not constitute an official endorsement or approval of the use thereof.

Destroy this report when it is no longer needed. Do not return it to the originator.

Army Research Laboratory
Adelphi, MD 20783-1197

ARL-TN-0548 **June 2013**

Model-Based Radar Power Calculations for Ultra-Wideband (UWB) Synthetic Aperture Radar (SAR)

Traian Dogaru
Sensors and Electron Devices Directorate, ARL

REPORT DOCUMENTATION PAGE

Form Approved
OMB No. 0704-0188

PLEASE DO NOT RETURN YOUR FORM TO THE ABOVE ADDRESS.

1. REPORT DATE *(DD-MM-YYYY)*	2. REPORT TYPE	3. DATES COVERED (From - To)
June 2013	Final	1/1/13

4. TITLE AND SUBTITLE

Model-Based Radar Power Calculations for Ultra-Wideband (UWB) Synthetic Aperture Radar (SAR)

5a. CONTRACT NUMBER

5b. GRANT NUMBER

5c. PROGRAM ELEMENT NUMBER

6. AUTHOR(S)

Traian Dogaru

5d. PROJECT NUMBER

5e. TASK NUMBER

5f. WORK UNIT NUMBER

7. PERFORMING ORGANIZATION NAME(S) AND ADDRESS(ES)

U.S. Army Research Laboratory
ATTN: RDRL-SER-U
2800 Powder Mill Road
Adelphi, MD 20783-1197

8. PERFORMING ORGANIZATION REPORT NUMBER

ARL-TN-0548

9. SPONSORING/MONITORING AGENCY NAME(S) AND ADDRESS(ES)

10. SPONSOR/MONITOR'S ACRONYM(S)

11. SPONSOR/MONITOR'S REPORT NUMBER(S)

12. DISTRIBUTION/AVAILABILITY STATEMENT

Approved for public release; distribution unlimited.

13. SUPPLEMENTARY NOTES

14. ABSTRACT

In this study, we establish a relationship between the radar transmitted power, the target signature and the signal-to-noise ratio required for a specific target detection performance in a radar system. While this relationship can be easily derived from the radar equation in the case of narrowband waveforms, this technical note extends the analysis to wideband waveforms and applies it to synthetic aperture radar systems as well. The technique is demonstrated though a numerical example, where computer data modeling a three-dimensional building imaging radar system is used in evaluating the radar transmitted power for a given target detection performance.

15. SUBJECT TERMS

ultra-wideband radar, synthetic aperture radar

16. SECURITY CLASSIFICATION OF:			17. LIMITATION OF ABSTRACT	18. NUMBER OF PAGES	19a. NAME OF RESPONSIBLE PERSON
a. REPORT	b. ABSTRACT	c. THIS PAGE			Traian Dogaru
Unclassified	Unclassified	Unclassified	UU	22	19b. TELEPHONE NUMBER (*Include area code*) (301) 394-1482

Standard Form 298 (Rev. 8/98)
Prescribed by ANSI Std. Z39.18

Contents

List of Figures

1. Introduction

The radar modeling team at the U.S. Army Research Laboratory (ARL) has developed a suite of simulation tools and methodologies that have been successfully applied to predict radar system performance in complex scenarios. Among these scenarios are ground penetrating radar and forward-looking radar for landmine and improvised explosive device detection, as well as sensing through the wall (STTW) radar for detection of targets inside buildings.

In general, the main focus of our modeling work has been on high-resolution imaging applications of an ultra-wideband (UWB) synthetic aperture radar (SAR). Specific to this sensing modality is the large range of frequencies and aspect angles for the data collection—in the simulation domain, that translates to a large amount of computational resources. An example of a large-scale radar simulation that creates the three-dimensional (3-D) image of a one-story building was reported in reference 1.

One limitation of our current models is that they emphasize the target scattering aspects and mostly ignore other important parameters of the radar system, such as antenna gain, system losses, receiver noise figure, etc. In some cases (far-field scenarios), the models even ignore the propagation (path) losses incurred by the radar waves. Additionally, by design, the electromagnetic (EM) scattering models do not include any external noise or radio frequency (RF) interference (which can actually have a significant impact on the performance of an UWB radar). However, in evaluating the overall radar performance, most of these effects can be accounted for in the post-processing of EM scattering model data.

This study attempts to partially fill this gap, by making the connection between quantities obtained via computer modeling (such as the target scattering parameters) and the more traditional radar system parameters, such as transmitted power and signal-to-noise ratio (SNR). More specifically, we evaluate the required peak transmitted power of the radar, based on the target scattering parameters and the level of SNR required for a specific target detection performance. We apply this method to UWB SAR imaging scenarios, where knowledge of the target response over a large range of frequencies and aspect angles is necessary. It is important to mention that the equations are valid regardless of the method employed in obtaining the target scattering parameters (which can be measurement-based as well as model-based).

The technical note is organized as following: section 2 discusses the theoretical aspects of the radar power calculation based on computer models, section 3 presents a numerical example, and section 4 offers conclusions.

2. Theoretical Calculation of the Radar Transmitted Power

2.1 Narrowband Radar, Far-Field Case

Throughout this study, we make the distinction between near-field and far-field radar-target configurations. While we do not discuss the specific quantitative criteria that separates the two cases (more details can be found in reference 2), we mention that the far-field assumption allows us to use the radar equation (*3*) for power calculation, whereas in the near-field case, the model on which the classic radar equation is derived, is generally not valid.

In this section, we consider a narrowband radar (with a bandwidth much smaller than the carrier frequency), operating in a far-field, monostatic configuration, with identical transmitter and receiver antennas. A simple form of the radar equation is the following (*3*):

$$P_r = \frac{P_t G^2 \lambda^2 \sigma}{(4\pi)^3 R^4} \ , \tag{1}$$

where P_r is the received power, P_t the peak transmitter power, G the antenna gain, λ the wavelength of the carrier, σ the radar cross section (RCS) of the target, and R the radar-target range. Throughout this study, the target is considered stationary.

In the following, we ignore certain factors that usually appear in the radar equation, such as system losses and receiver noise figure (*3*). We also assume that the detection is performed based on a single transmitted pulse (no pulse integration performed), by comparing the magnitude of a post-detection sample within the range gate of the target with a threshold. The effect of system losses, receiver noise figure, and pulse integration can be accounted for by adding corresponding factors to the radar equation; however, their omission does not change the principle of the method outlined here.

Computer programs that model radar far-field scattering scenarios, such as AFDTD (*4*), FEKO (*5*), or Xpatch (*6*), perform calculations of the complex target scattering parameter *S*, which links the electric field intensities incident to and scattered by the target (for a more precise definition, see reference 7). The relationship between S and σ is $\sigma = 4\pi|S|^2$.

Throughout this note, we assume that the radar performance is limited by the thermal noise at the receiver antenna (*3*), so we ignore other sources of noise or interference. The thermal noise is usually modeled as having a constant power spectral density (PSD) in the band of interest, equal to $k_B T_0$, where k_B is Boltzmann's constant and T_0 is the temperature. The average power of the noise is then $k_B T_0 B$, where B is the receiver noise bandwidth (which we assume equal to the transmitted pulse bandwidth).

Now assume that we require a specific SNR for a desired target detection performance. Then we formulate our problem as following: given the *S* parameter calculated via the computer model, find the transmitter power P_t in order to obtain the specified SNR. For this, we write the SNR as

$$\text{SNR} = \frac{P_r}{k_B T_0 B} = \frac{P_t G^2 \lambda^2 |S|^2}{(4\pi)^2 R^4 k_B T_0 B}. \quad (2)$$

From here, we derive

$$P_t = \frac{(4\pi)^2 R^4 k_B T_0 B(\text{SNR})}{G^2 \lambda^2 |S|^2}. \quad (3)$$

2.2 Wideband Radar, Far-Field Case

The calculations in the previous section are valid for a transmitted radar signal with a narrow bandwidth (long duration). Now we consider the case of a wideband pulse, which typically has a short duration. For the present discussion, we assume that the pulse consists of an amplitude-modulated (AM) carrier, and no pulse compression technique (*3*) is used (the pulse compression case is mentioned briefly at the end of this section). A typical relationship between duration and bandwidth for such a pulse is (*3*) $\tau \cong 1/B$. In this study, we work with discrete (sampled) signals in both time and frequency domains. The conversion of signals from one domain to the other can be made via discrete Fourier transforms (DFTs), which involve sequences of length *N* in both domains. Notice that *N* is also indicative of the number of range resolution cells covered by the receiver time gate (time when the receiver is turned on), as well as the number of samples collected by the receiver during that time (assuming time domain sampling at Nyquist rate [*8*]).

We further assume that the spectral content of the transmitted pulse is relatively flat over the signal bandwidth. Then, the magnitude of each of the *N* spectral component equals the transmitted pulse peak power (defined as the average power of the pulse over its duration; this should not be confused with the average transmitted power of the radar, where the average is calculated over a pulse repetition interval). The radar equation can be written separately for each spectral component (indexed by *k*, with *k* from 1 to *N*) as

$$P_{r,k} = \frac{P_t G_k^2 \lambda_k^2 |S_k|^2}{(4\pi)^2 R^4}. \quad (4)$$

Notice that in equation 4 we used the index *k* for *G*, λ, and *S*, to represent the fact that they vary with frequency. However, the value of P_t was considered constant over the bandwidth.

Next we consider the signal at the receiver, which is made of a target-scattered component and an additive noise component. For the former, we call the power of each time-domain sample $p_{r,n}$, and the power of each frequency-domain component $P_{r,k}$, with indexes *n* and *k* running from 1 to *N*. For the latter, we call the power of the time-domain samples w_n, and the power of

the frequency-domain components W_k. We define the SNR of the received signal as the ratio of the average time-domain target-scattered sample to the average time-domain noise sample. Now, it is reasonable to assume that the target response extends over M resolution cells, with $M < N$. Then, we compute the SNR as the average SNR over those M resolution cells.

Using Parseval's theorem (*8*) and the fact that the average power of a time-domain noise sample is $k_B T_0 B$, we obtain

$$\text{SNR} = \frac{\frac{1}{M}\sum_{n=1}^{M} p_{r,n}}{\frac{1}{M}\sum_{n=1}^{M} w_n} = \frac{\frac{1}{M}\sum_{n=1}^{N} p_{r,n}}{\frac{1}{M}\sum_{n=1}^{M} w_n} = \frac{\sum_{k=1}^{N} P_{r,k}}{NMk_B T_0 B}. \tag{5}$$

In the above equation, we used the following discrete version of Parseval's theorem:

$$\sum_{n=1}^{N} p_{r,n} = \frac{1}{N}\sum_{k=1}^{N} P_{r,k}, \tag{6}$$

as well as the fact that the $p_{r,n}$ samples are zero outside the M resolution cells that make up the target response. It is very important to emphasize that, in equation 5, we compute the SNR strictly over the spatial extent of the target response—we cannot use the SNR over the entire range swath sensed by the radar (corresponding to N resolution cells), or the SNR over one particular resolution cell either.

Finally, from equations 4 and 5, we can derive the required transmitted peak power for a given SNR:

$$P_t = \frac{(4\pi)^2 R^4 k_B T_0 B(\text{SNR})NM}{\sum_{k=1}^{N} G_k^2 \lambda_k^2 |S_k|^2}. \tag{7}$$

In general, M can be computed as

$$M = \frac{\Delta R}{\delta R} = \frac{2B\Delta R}{c}, \tag{8}$$

where ΔR is the target extent in range, and δR is the range resolution. Notice that the case when $M = N$ corresponds to a frequency-domain sampling of the S_k sequence at the Nyquist rate (the receiver time gate corresponds directly to the range extent of the target response). An interesting conclusion we draw from equation 7 is that there is no advantage or disadvantage in increasing the width of the receiver time gate (or, equivalently, increasing N), since both the numerator and the denominator in the expression of the transmitted power increase by a proportional amount (the denominator via the sum from 1 to N).

The peak power of the transmitted signal can be brought down significantly if a pulse compression scheme is employed (*3*). For such a pulse, the product between duration τ and bandwidth *B* (also known as the compression ratio [CR]) is much larger than the unity (a typical value would be 100). In this case, the required transmitted peak power is reduced by a factor CR (*9*):

$$P_t = \frac{(4\pi)^2 R^4 k_B T_0 B(\mathrm{SNR}) NM}{(\mathrm{CR})\sum_{k=1}^{N} G_k^2 \lambda_k^2 |S_k|^2} = \frac{(4\pi)^2 R^4 k_B T_0 (\mathrm{SNR}) NM}{\tau \sum_{k=1}^{N} G_k^2 \lambda_k^2 |S_k|^2}. \quad (9)$$

Notice that the final form of equation 9 is valid in general for any type of pulse, regardless of whether compression is used or not.

2.3 Wideband SAR, Far-Field Case

In this section, we consider the model of a SAR imaging scenario, where the EM simulation program computes the *S* parameters (or received signal) over a range of frequencies and aspect angles. To be more specific, we consider a circular spotlight SAR data collection geometry (*10*), where the radar operates monostatically in the far-field. For now, we analyze a two-dimensional (2-D) imaging geometry; a 3-D imaging geometry example is shown in section 3.

The derivation of the transmitted peak power for this case largely follows the procedure in section 2.2, with the difference that we now work with 2-D (sampled) signals, both in spatial (or image) and frequency-angle domains. As shown in reference 10, a 2-D Fourier transform relationship can be established between the signals in the two domains. The EM simulation software computes the received 2-D signals in the frequency-angle domain. The SAR image can then be interpreted as a 2-D inverse Fourier transform of these data samples (details of the numerical calculation of this Fourier transform are not trivial, but are not discussed here).

Without going again through every step as in section 2.2, we mention that the data in the frequency-angle domain are transformed to the image domain, and the image SNR for a desired target detection performance is found. As previously, we emphasize the fact that the SNR is computed as an average of the signal power to the average noise power over the target image extent, which is assumed to comprise M_D resolution cells in down-range and M_C resolution cells in cross-range.

By analogy with the one-dimensional case presented in section 2.2, the equation that expresses the total peak power transmitted by the radar to obtain an image with a given SNR is

$$P_t^{total} = \frac{(4\pi)^2 R^4 k_B T_0 B(\mathrm{SNR}_{image}) NLM_D M_C}{\sum_{k=1}^{N}\left(\sum_{l=1}^{L}|S_{k,l}|^2\right) G_k^2 \lambda_k^2}. \quad (10)$$

where l is the aspect angle index that runs from 1 to L; also, no pulse compression was considered here. The antenna gain G depends on frequency only for the spotlight SAR mode. However, if we want to adapt this equation to a strip-map data collection geometry (*10*), we may need to take into account the gain variation with angle as well (if this variation is significant within the angular range employed in the image formation algorithm).

To compute the peak power of one transmitted pulse (or the peak power of the radar), we need to take into account that L pulses are employed in creating the SAR image. That means the peak power of one individual pulse is P_t^{total} divided by L, or

$$P_t = \frac{(4\pi)^2 R^4 k_B T_0 B(\mathrm{SNR}_{image}) N M_D M_C}{\sum_{k=1}^{N}\left(\sum_{l=1}^{L}\left|S_{k,l}\right|^2\right) G_k^2 \lambda_k^2}. \tag{11}$$

Notice in equation 11 that increasing the number of data collection points along the synthetic aperture (L) helps to bring down the transmitter power for a given image SNR (via increasing the number of terms in the sum from 1 to L that appears in the denominator), or, equivalently, increases the image SNR for a fixed transmitter power.

2.4 Near-Field Case

For a near-field radar scattering scenario, the direct application of the radar equation is not valid any longer, since some of the quantities and concepts used in its derivation only make sense for far-field geometries. Moreover, the equation connecting the transmitted and received radar powers depends strongly on the type of radar antennas, and in most cases, cannot be expressed in analytic form. Even when this connection is evaluated via EM computer models, there is no standardized way of implementing the transmitter and receiver antennas or characterizing the target scattering (by comparison, the S parameter for the far-field case is a well-defined quantity and does not depend on the evaluation method).

Despite these difficulties, we derive the equation of the peak transmitted power for the case when the near-field radar scenario is simulated with the NAFDTD software (*11*), and the transmitter and receiver antennas are provided by infinitesimal dipoles. We first consider the narrowband case. According to the theory of this type of antennas (*2*), we have

$$P_t = Z_0 \frac{\pi}{3} \frac{\left|I_0 l\right|^2}{\lambda^2}, \tag{12}$$

$$P_r = \frac{\left|E_r\right|^2}{2Z_0} \frac{3\lambda^2}{8\pi}, \tag{13}$$

where Z_0 is the free-space impedance, $I_0 l$ is the current moment of the transmitter (*2*), and E_r is the electric field at the location of the receiving dipole. The NAFDTD program computes the

target response for an excitation with $I_0 l = 1$; let us call the field at the receiver in this case E_r^0. Then, for a general excitation, we have

$$P_t = Z_0 \frac{\pi}{3\lambda^2} \frac{\left|E_r\right|^2}{\left|E_r^0\right|^2}. \tag{14}$$

At the same time, the SNR can be written as

$$\text{SNR} = \frac{P_r}{k_B T_0 B} = \frac{\left|E_r\right|^2 3\lambda^2}{16\pi Z_0 k_B T_0 B}. \tag{15}$$

By extracting $\left|E_r\right|^2$ from the last equation and replacing it in equation 14, we obtain

$$P_t = \frac{(4\pi)^2 Z_0^2 k_B T_0 B(\text{SNR})}{9\lambda^4 \left|E_r^0\right|^2}. \tag{16}$$

Notice that, as compared to equation 3, this expression does not explicitly contain parameters such as the antenna gain *G* and the range *R*. This is because, unlike the *S* parameter (from the far-field case), the E_r^0 parameter implicitly contains all the other factors.

Now let us extend the method to an UWB SAR scenario. In this case, we assume that the radar moves along a certain trajectory and measures the target response from *L* pairs of transmitter-receiver locations. Let us call $E_{r,k,l}^o$ the field at the receiver computed by the NAFDTD code, for frequency index *k* and radar location index *l*. Then, by applying arguments similar to those in section 2.3, we obtain

$$P_t = \frac{(4\pi)^2 Z_0^2 k_B T_0 B(\text{SNR}_{image}) N M_D M_C}{9\sum_{k=1}^{N}\left(\sum_{l=1}^{L}\left|E_{r,k,l}^0\right|^2\right)\lambda_k^4}. \tag{17}$$

3. Numerical Example

In this section, we present a numerical example demonstrating how to estimate the peak power required by a STTW radar system in order to obtain 3-D images of a building with a given SNR metric. The calculations are related to the work in reference 1, where the 3-D images were obtained from simulated radar data. The building has a single floor and contains four stationary human targets (figure 1). For this study, we assume an airborne radar system, placed in the far-field, and collecting data in a circular spotlight mode over certain ranges of azimuth and elevation angles from one side of the building (figure 2). The 3-D image obtained for vertical-

vertical (V-V) polarization is shown in figure 3, where we represent only the output of a constant false alarm rate (CFAR) detector.

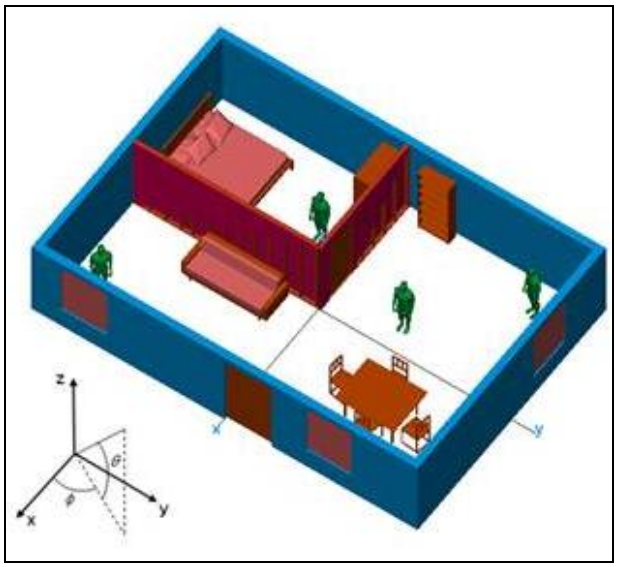

Figure 1. Description of the single-story building used in the 3-D radar image study.

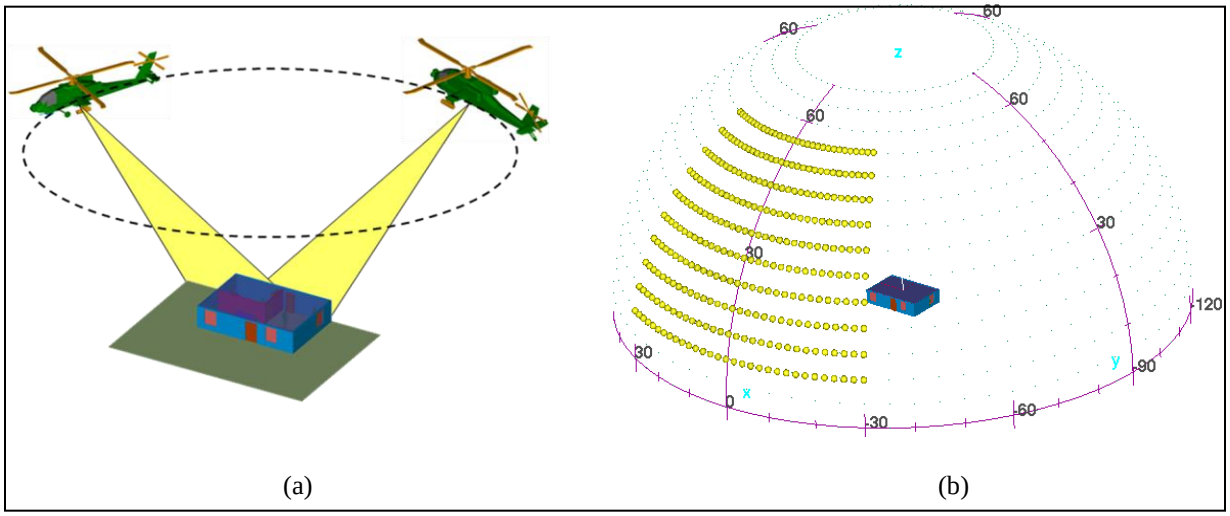

Figure 2. Schematic representations of the airborne spotlight radar imaging system, showing (a) the radar platform moving in a circular pattern around the building and (b) the synthetic aperture positions (marked as yellow dots) placed on a sphere.

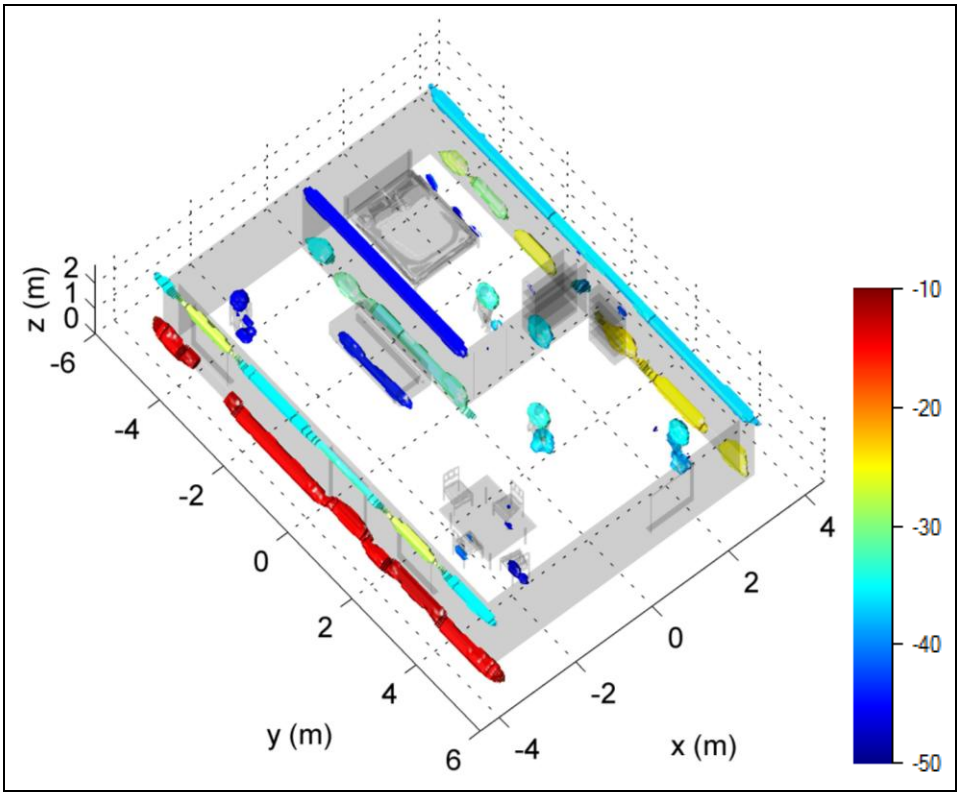

Figure 3. The 3-D building image for the airborne spotlight configuration and V-V polarization. The feature colors correspond to their brightness levels in the raw 3-D image.

To obtain the image in figure 3, a certain amount of complex-valued white Gaussian noise was added to the data directly in the image domain. The noise average power is taken relative to the maximum intensity voxels (in our case, these can be found along the lower edge of the front wall). By inspecting the image in figure 3 we find that the strongest feature (the lower edge of the front wall) has a power of –10 dB, while the weakest feature that we want to detect (the human closest to the front wall) has a power of about –50 dB. In a typical detector, the target would need to be about 10 dB above the average noise level in order to pass the detection test, meaning that the noise average power should be –60 dB. This gives us a ratio between the maximum intensity voxel and the noise average power of –50 dB.

Now, according to the discussion in section 2.3, we recognize that this power ratio (which ultimately determines the radar system performance in detecting the human targets) is not the same quantity as the image SNR used in equation 11. Instead, as an intermediate step, we need to numerically compute the average SNR over all the image voxels, when the image noise average power is –60 dB (as determined in the previous paragraph). This calculation yields SNR_{image} = 15 dB.

Equation 11 can be adapted to a 3-D imaging geometry as follows:

$$P_t = \frac{(4\pi)^2 R^4 k_B T_0 B(\mathrm{SNR}_{image}) N M_D M_C M_E}{\sum_{k=1}^{N}\left(\sum_{l=1}^{L}\sum_{q=1}^{Q}\left|S_{k,l,q}\right|^2\right) G_k^2 \lambda_k^2}, \tag{18}$$

where this time the S parameters are computed over three dimensions (q indicates the elevation angle index), while M_D, M_C and M_E represent the numbers of resolution cells within the image, in down-range, cross-range, and elevation range, respectively. These numbers can be computed according to the following formulas (see reference 1):

$$M_D = \Delta DR \frac{2B_{eff}}{c}, \tag{19}$$

$$M_C = \Delta CR \frac{4 f_0 \sin\frac{\Delta\phi_{eff}}{2}}{c}, \tag{20}$$

$$M_E = \Delta ER \frac{4 f_0 \sin\frac{\Delta\theta_{eff}}{2}}{c}. \tag{21}$$

In these equations, we used the following notations:

ΔDR – the image dimension in down-range (along x-axis)

ΔCR – the image dimension in cross-range (along y-axis)

ΔER – the image dimension in elevation range (along z-axis)

B_{eff} – the effective bandwidth of the radar data

$\Delta\phi_{eff}$ – the effective azimuth angle range for the radar data

$\Delta\theta_{eff}$ – the effective elevation angle range for the radar data

f_0 – the center frequency for the radar data

c – the speed of light

In the numerical study performed in reference 1, the following parameters were used: B = 2.2 GHz, f_0 = 1.4 GHz, B_{eff} = 1.1 GHz, $\Delta\phi_{eff}$ = 15°, $\Delta\theta_{eff}$ = 20°, ΔDR = 9 m, ΔCR = 12 m, ΔER = 2.75 m, N = 331. Additionally, we assume that R = 1 km and the antenna gain is given by

$$G(f) = 10^{[(f-0.3)/4.4+0.5]}, \tag{22}$$

where f is the frequency in GHz. This expression indicates that the antenna gain varies between 5 and 10 dBi in the frequency band of interest, which is typical for a SAR system operating in

the spotlight mode at those frequencies. The total power of the scattering parameters S (added over all three data dimensions) is 6.8×10^{6} square-meters. For the $k_B T_0$ constant we take the usual value of 4×10^{-21} J.

After plugging all these parameters in equation 10, we obtain P_t = 20 kW. This is an unreasonably high value for the transmitted peak power in an airborne radar system. However, this figure assumes that we do not use any pulse compression technique. As mentioned in section 2.2, if we use pulse compression, the peak power is reduced by a factor proportional to the compression ratio. For instance, for CR = 100, we obtain P_t = 200 W, which is a more manageable figure. In fact, most airborne radar systems employ some kind of pulse compression technique in order to keep the peak power to low values. Also, keep in mind that the peak power calculation is very sensitive to the choice of the range R; thus, operating the radar at smaller ranges can dramatically reduce the required transmitted power.

One caveat regarding this calculation is the fact that the 3-D images created in reference 1 are not based on the received radar signals, but on the S-parameters. The received signals differ from the S-parameters by a scaling factor that can be easily derived from the radar equation. As long as this scaling factor does not depend on frequency and aspect angle, the two images (obtained from the two sets of data) are simply scaled up/down versions of one another. Since the only way the power of the image voxels appears in the radar peak power expression is through SNR_{image}, scaling up or down the image intensity by a factor does not change the final calculation. However, the scaling factor that links the received signals to the S-parameters generally depends on frequency through the antenna gain G and the wavelength λ; therefore, the SAR images based on the two sets of data may look slightly different, which can, in turn, lead to different values of the peak transmitted power. This issue can be resolved by re-creating the images with a set of corrected S-parameters that account for the variation of G and λ with frequency. Nevertheless, we did not pursue this procedure in this study, which is only meant to illustrate the general method for peak power calculation.

4. Conclusions

In this note, we derived equations for the radar peak transmitted power as a function of radar system parameters, the target scattering strength and the desired SNR at the output of the radar processing chain. The method was applied to SAR images obtained by UWB radar. The target scattering is characterized by the scattering parameters S (whose magnitude square is equivalent to the target RCS), with this quantity determined separately by computer simulations or measurements. For UWB SAR systems, an important fact is that S depends on both frequency and aspect angle. In sections 2.2 and 2.3 we paid particular attention to the way we define the

SNR that appears in the final equation of the peak power, as well as the number of resolution cells that need to be considered in the calculation.

The theoretical derivations were followed by a numerical example that applies the method to estimate the peak power of an airborne radar that creates the 3-D image of a building. The desired SNR level is based on the requirement that we detect all four human targets inside the building. The large peak power obtained from this calculation for unmodulated pulses underscores the challenges faced by any STTW radar system, where the target signature is severely attenuated by the round-trip through-wall transmission of the radar waves. It also justifies the need to use a pulse compression technique in order to keep the peak transmitter power down.

In this example, we assumed that the radar detection performance is limited by thermal noise. However, in a scenario involving through-the-wall detection of stationary targets, the performance is most likely limited by other factors such as clutter, image sidelobes and multipath propagation, and scattering. Nevertheless, these issues cannot be mitigated by increasing the transmitted power, but instead by the correct choice of imaging geometry and advanced signal processing algorithms.

5. References

1. Dogaru, T.; Liao, D.; Le, C. *Three-Dimensional Imaging of a Building*; ARL-TR-6295; U.S. Army Research Laboratory: Adelphi, MD, December 2012.
2. Balanis, C. *Antenna Theory – Analysis and Design*; Wiley: New York, 1997.
3. Skolnik, M. I. *Introduction to Radar Systems*; McGraw Hill: New York, 2001.
4. Dogaru, T. *AFDTD User's Manual*; ARL-TR-5145; U.S. Army Research Laboratory: Adelphi, MD, March 2010.
5. FEKO EM Simulation Software Web page. http://www.feko.info (accessed October 2011).
6. Science Applications International Corporation (SAIC) Web page. http://www.saic.com/products/software/xpatch (accessed December 2011).
7. Ruch, G.; Barrick, D. E.; Stuart, W. D.; Krichbaum, C. K. *Radar Cross Section Handbook*; Plenum Press: New York, 1970.
8. Oppenheim, A. V.; Schafer, R. W. *Discrete-time Signal Processing*; Prentice Hall: Englewood Cliffs, NJ, 1989.
9. Mahafza, B. R. *Radar Systems Analysis and Design Using MATLAB*; CRC Press: Boca Raton, FL, 2005.
10. Soumekh, M. *Synthetic Aperture Radar Signal Processing*; Wiley: New York, 1999.
11. Dogaru, T. *NAFDTD – A Near-Field Finite Difference Time Domain Solver*; ARL-TR-6110; U.S. Army Research Laboratory: Adelphi, MD, September 2012.

List of Symbols, Abbreviations, and Acronyms

2-D	two-dimensional
3-D	three-dimensional
AM	amplitude modulation
ARL	U.S. Army Research Laboratory
CFAR	constant false alarm rate
CR	compression ratio
DFT	discrete Fourier transform
EM	electromagnetic
PSD	power spectral density
RCS	radar cross section
RF	radio frequency
SAR	synthetic aperture radar
SIRE	Synchronous Impulse Reconstruction
SNR	signal to noise ratio
STTW	sensing through the wall
UWB	ultra-wideband
V-V	vertical-vertical

No. of Copies	Organization
1 (PDF)	DEFENSE TECHNICAL INFORMATION CTR DTIC OCA
10 (PDFS)	US ARMY RSRCH LAB ATTN IMAL HRA MAIL & RECORDS MGMT ATTN RDRL CIO LL TECHL LIB ATTN RDRL SER U M RESSLER (1 PDF) A SULLIVAN (1 PDF) C LE (1 PDF) K RANNEY (1 PDF) L NGUYEN (1 PDF) D LIAO (1 PDF) K SHERBONDY (1 PDF) T DOGARU (1 PDF)

INTENTIONALLY LEFT BLANK.